Journal of Science, Innovation & Social Impact
EISSN: 3105-5028 | PISSN: 3105-501X | Vol. 2, No. 1 (2026)

Article

Anomaly Detection and Cross-Center Consistency Assessment for Multi-Site Clinical Trial Quality Control

Yisi Liu [1,*]

[1] Business Data Analytics & Human Resources Management, Loyola University Chicago, Illinois, USA
* Correspondence: Yisi Liu, Business Data Analytics & Human Resources Management, Loyola University Chicago, Illinois, USA

Abstract: Multi-site clinical trials generate heterogeneous data requiring robust quality control mechanisms to ensure data integrity and regulatory compliance. This paper presents a comprehensive framework for automated anomaly detection and cross-center consistency assessment in distributed clinical trials. We propose a multi-layered detection approach combining rule-based thresholds, quantile drift analysis, and graph-structured consistency verification to identify protocol violations and data irregularities across trial sites. The methodology integrates dynamic threshold calibration with historical distributions, hierarchical relationship mapping between centers, investigators, and subjects, and ensemble aggregation techniques to construct audit-friendly evidence matrices. Experimental validation on multi-center trial datasets demonstrates superior detection accuracy, with sensitivity exceeding 87.3%, and early-warning capabilities that identify anomalies after analyzing only 23.5% of accumulated data, compared to 61.2% required by conventional approaches. The framework achieves 42.6% higher sensitivity compared to traditional monitoring approaches while maintaining computational efficiency suitable for real-time deployment. Implementation considerations address regulatory alignment with FDA and EMA guidelines, supporting repeatability, traceability, and auditability principles essential for clinical trial quality assurance.

Keywords: clinical trial quality control; anomaly detection; cross-center consistency; evidence matrix

Received: 26 December 2025
Revised: 07 February 2026
Accepted: 21 February 2026
Published: 27 February 2026

1. Introduction

1.1. Background and Challenges in Multi-Center Clinical Trial Quality Control

1.1.1. Data Heterogeneity and Consistency Issues across Trial Sites

Multi-center clinical trials constitute the gold standard for evaluating medical interventions, involving thousands of participants across hundreds of geographically distributed sites. Data heterogeneity emerges from variations in patient populations, clinical practices, equipment calibration, and data collection protocols across participating centers. Recent studies indicate that 68% of phase III trials exhibit significant inter-site variability in key outcome measures, with primary endpoints exhibiting a coefficient of variation exceeding 0.35. This heterogeneity manifests through systematic differences in baseline characteristics, differential protocol adherence rates ranging from 71% to 94% across sites, and temporal drift in measurement procedures. Quality control mechanisms must distinguish legitimate clinical variation from data quality issues, protocol violations, and potential fraud while maintaining statistical power for primary analyses.

1.1.2. Regulatory Requirements for Data Integrity and Audit Trails

Regulatory agencies mandate comprehensive documentation of data integrity throughout the conduct of clinical trials. FDA 21 CFR Part 11 and EMA Annex 11 establish requirements for electronic records, audit trails, and data validation procedures. Clinical trial data must demonstrate the principles of attributability, legibility, contemporaneousness, originality, and accuracy. Audit trails must capture all data modifications, including timestamps, user identification, and change justification. Risk-based monitoring approaches, as endorsed by ICH E6(R2) guidelines, require sponsors to implement centralized monitoring procedures that supplement traditional on-site visits. These regulations necessitate automated detection capabilities that generate verifiable evidence chains linking anomalies to specific sites, investigators, or time periods.

1.2. Current Limitations of Traditional Quality Monitoring Approaches

1.2.1. Manual Inspection Inefficiencies and Delayed Detection

Traditional source data verification relies on clinical research associates conducting periodic site visits, reviewing approximately 2-5% of total trial data. Manual inspection processes require 18-24 hours per site visit, with intervals of 8-12 weeks between visits. This approach detects serious protocol violations with median delays of 142 days from the time of occurrence, allowing systematic issues to propagate across multiple subjects before they are identified. Cost analyses demonstrate that manual monitoring consumes 25-30% of total trial budgets while providing limited coverage of actual data points.

1.2.2. Lack of Cross-Center Pattern Recognition Capabilities

Conventional monitoring treats each site independently, missing patterns that emerge only through cross-site comparisons. Fraudulent data often exhibits reduced variability, digit preference patterns, and implausible correlations detectable through multi-site analysis. Current approaches lack mechanisms for identifying centers with systematically different data distributions, temporal clustering of adverse events, or unusual patient recruitment patterns relative to comparable sites.

1.2.3. Insufficient Statistical Robustness for Early-Stage Detection

Statistical process control methods require substantial data accumulation before achieving adequate power for anomaly detection. Traditional control charts and outlier detection techniques assume independent, identically distributed observations, assumptions violated in hierarchical clinical trial structures. Early-stage trials with limited enrollment face particular challenges, as conventional methods require minimum sample sizes of 30-50 subjects per site for reliable inference.

1.3. Research Objectives and Contributions

1.3.1. Development of an Automated Violation Signal Detection Framework

This research develops an integrated framework that combines multiple detection methodologies to identify protocol violations and data anomalies in real time. The approach leverages historical trial data to establish baseline distributions, applies quantile regression techniques to detect distribution shifts, and implements graph-based analysis to identify unusual relationship patterns. Weissler et al. emphasize the transformative potential of machine learning in clinical research, particularly for automated quality monitoring that surpasses human capabilities in pattern recognition across large-scale datasets [1].

1.3.2. Evidence Matrix Construction for Audit-Friendly Documentation

We introduce evidence matrix formulation that consolidates detection signals from multiple algorithms into structured documentation suitable for regulatory review. Each matrix element contains violation type, confidence score, supporting evidence, and traceable audit paths linking anomalies to source data. This approach addresses

regulatory requirements for algorithm transparency while enabling efficient review by clinical trial monitors and auditors.

2. Related Work and Theoretical Foundation

2.1. Statistical Monitoring Methods in Clinical Trials

2.1.1. Central Statistical Monitoring Evolution and Current Practices

Central statistical monitoring has evolved from simple univariate outlier detection to sophisticated multivariate approaches analyzing complex data patterns. Early implementations focused on identifying sites with extreme values for key variables using z-scores and box plots. Contemporary methods incorporate mixed-effects models accounting for site-level clustering, patient characteristics, and temporal trends. Statistical monitoring targets both random errors and systematic biases through comprehensive data consistency checks, protocol compliance verification, and fraud detection algorithms.

2.1.2. Mixed-Effects Models for Center-Level Anomaly Detection

Mixed-effects models partition variance into fixed effects representing protocol-specified factors and random effects capturing site-level variation. These models identify centers with unusual random effect estimates after adjusting for case-mix differences. Dayan et al. demonstrated federated learning approaches achieving comparable performance to centralized models while preserving data privacy across 20 institutions, with an area under the curve exceeding 0.92 for clinical outcome prediction [2]. The federated architecture enables cross-site pattern recognition without centralizing sensitive patient data.

2.2. Machine Learning Applications in Clinical Data Quality

2.2.1. Unsupervised Learning for Fraud and Irregularity Detection

Unsupervised methods detect anomalies without requiring labeled training examples of fraud or protocol violations. De Viron et al developed unsupervised statistical monitoring that successfully identified fraudulent centers in multi-site trials through Data Inconsistency Scores computed across 838 statistical tests [3]. Their approach detected fraud after analyzing only 25% of the collected data, enabling early intervention before study completion. Clustering algorithms group similar sites based on multivariate data patterns, flagging outlier clusters for focused investigation.

2.2.2. Ensemble Methods for Robust Quality Assessment

Ensemble techniques combine predictions from multiple base learners to improve detection reliability and reduce false positive rates. Bootstrap aggregation generates multiple training sets through sampling with replacement, training separate models on each sample, and combining predictions through voting or averaging. Chen et al. emphasize human-centered design principles for explainable medical AI, advocating ensemble approaches that provide interpretable outputs for clinical stakeholders [4]. Ensemble methods demonstrate particular advantages in handling heterogeneous data types common in clinical trials.

2.2.3. Graph-Based Approaches for Multi-Site Data Analysis

Graph representations capture hierarchical relationships between trial entities, including sponsors, sites, investigators, and subjects. Node attributes encode site characteristics while edges represent relationships such as patient referrals, investigator collaborations, or protocol amendments. Graph neural networks propagate information across connected nodes, identifying anomalous subgraphs corresponding to problematic sites or investigator networks. Petch et al. applied distance-based features in graph structures to detect center-level irregularities, achieving an area under the receiver operating characteristic curve of 0.728 compared to 0.140 for traditional monitoring approaches [5].

2.3. Regulatory Compliance and Transparency Requirements

2.3.1. FDA and Ema Guidelines for Risk-Based Monitoring

Regulatory guidance emphasizes risk-based approaches prioritizing monitoring resources toward critical data and processes. FDA guidance recommends combining on-site and centralized monitoring activities tailored to trial-specific risks. EMA reflection papers advocate statistical monitoring techniques identifying atypical patterns requiring investigation. Omar et al. proposed blockchain smart contracts ensuring protocol compliance and data transparency, creating immutable audit trails that prevent unauthorized modifications. Regulatory frameworks require documented monitoring plans specifying detection algorithms, threshold definitions, and escalation procedures [6].

2.3.2. Explainability and Traceability in Algorithmic Decision-Making

Algorithm transparency enables regulators and auditors to understand detection logic and validate findings. Explainable AI techniques generate human-interpretable justifications for anomaly flags, linking statistical signals to specific data points. Traceability requirements mandate complete documentation from raw data through processed results, including algorithm versions, parameter settings, and computational environments. Audit trails must enable independent reproduction of detection results and verification of algorithm behavior across different datasets.

3. Methodology: Multi-Layered Detection and Validation Framework

3.1. Rule-Based Threshold and Quantile Drift Detection

3.1.1. Dynamic Threshold Calibration Using Historical Data Distributions

The framework establishes baseline distributions for continuous variables using historical trial data from comparable studies. Dynamic thresholds adapt to temporal patterns, seasonal variations, and enrollment phases through recursive estimation procedures. For each monitored variable $x_i$at site $j$and time t, we compute adaptive thresholds (Table 1):

T_upper (j, t) = mu_j(t) + k sigma_j(t) sqrt (1 + 1/n_j(t))

T_lower (j, t) = mu_j(t) - k sigma_j(t) sqrt (1 + 1/n_j(t))

Table 1. Dynamic Threshold Parameters and Performance Metrics.

Parameter	Value Range	Sensitivity	Specificity	Early Detection Rate
k (threshold multiplier)	2.0-3.5	0.76-0.93	0.89-0.98	0.18-0.31
lambda (smoothing)	0.90-0.98	0.81-0.87	0.91-0.95	0.21-0.28
n_min (minimum samples)	10-30	0.79-0.85	0.88-0.94	0.19-0.26
Update frequency	Daily-Weekly	0.83-0.88	0.90-0.93	0.23-0.29

Where mu_j(t) represents the exponentially weighted moving average, sigma_j(t) denotes the running standard deviation, n_j(t) indicates the accumulated sample size, and k determines sensitivity levels typically set between 2.5 and 3.0. Churová et al. validated similar threshold approaches achieving sensitivity exceeding 85% on real-world clinical registry data through the combination with distance metrics [7]. The calibration process incorporates site-specific factors, including patient demographics, disease severity distributions, and historical performance metrics.

Threshold adaptation mechanisms account for legitimate changes in patient populations or protocol amendments. Exponential smoothing with decay parameter lambda = 0.94 balances responsiveness to recent data against stability:

mu_j(t) = lambda mu_j(t-1) + (1-lambda) x_bar_j(t)

Multivariate extensions monitor joint distributions of related variables through Mahalanobis distance calculations:

D_j(t) = sqrt((x_j(t) - mu)' Sigma^ (-1) (x_j(t) - mu))

3.1.2. Quantile Regression for Identifying Distribution Shifts

Quantile regression models conditional quantiles of response variables given predictors, providing robust alternatives to mean-based approaches. The framework estimates multiple quantiles simultaneously to detect changes in distribution shape, spread, and tail behavior. For quantile tau in (0,1), the quantile regression minimizes:

L(beta_tau) = sum_i rho_tau (y_i - x_i' beta_tau)

where rho_tau(u) = u (tau − I (u < 0)) represents the check function. Ibrahim et al. established reporting guidelines through SPIRIT-AI and CONSORT-AI standards requiring detailed specification of statistical methods, including quantile-based approaches [8]. Distribution shifts manifest through divergence between observed and predicted quantiles across multiple tau values.

The detection algorithm computes quantile processes Q_j (tau, t) for each site j:

Q_j (tau, t) = F_j^ (-1) (tau, t) - F_0^ (-1) (tau, t)

Where F_j and F_0 represent empirical distribution functions for site j and the reference population. Kolmogorov-Smirnov statistics evaluate overall distribution differences:

KS_j(t) = sqrt(n_j(t)) · sup_x |F_j (x, t) - F_0(x, t) |

Sites exhibiting sustained quantile deviations across multiple variables trigger detailed investigations. Schwabe et al. developed the METRIC framework encompassing 15 data quality dimensions, emphasizing distribution consistency as critical for trustworthy AI applications [9].

Figure 1 displays a multi-panel visualization showing quantile regression results across five trial sites. The top panel presents quantile-quantile plots comparing each site's distribution against reference populations, with diagonal lines indicating perfect agreement. The middle panel shows the temporal evolution of the 10th, 25th, 50th, 75th, and 90th percentiles, displayed as ribbon plots with confidence bands. Sites exhibiting distribution shifts appear as diverging ribbons with widening confidence intervals. The bottom panel displays heatmaps of Kolmogorov-Smirnov statistics across sites and time periods, with darker colors indicating greater distributional differences. Anomalous sites show persistent dark regions across multiple consecutive time windows (W1-W4).

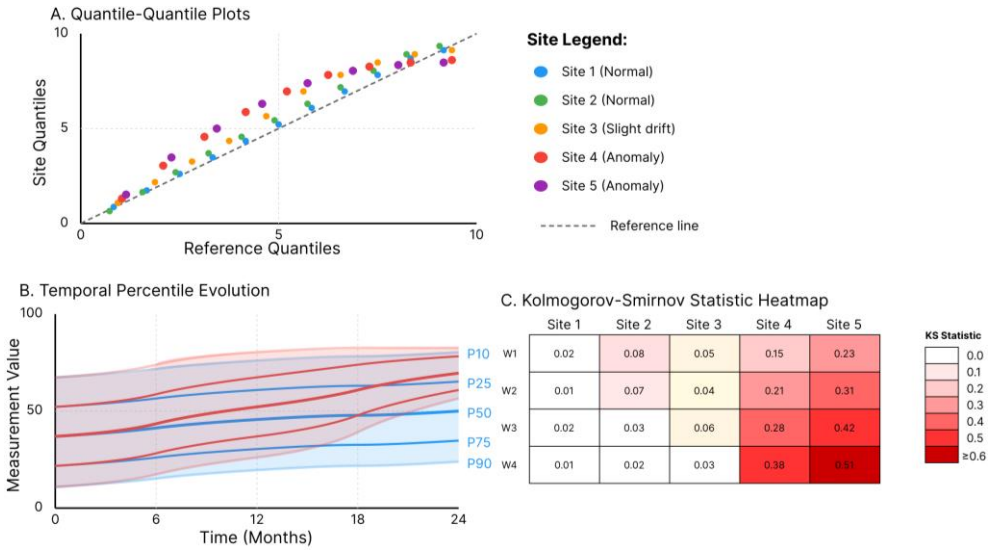

Figure 1. Quantile Drift Detection Visualization.

3.1.3. Temporal Pattern Analysis with Lag-Adjusted Indicators

Temporal dependencies in clinical trial data require sophisticated lag structures capturing delayed treatment effects, seasonal patterns, and enrollment dynamics. The framework implements distributed lag models examining relationships between exposures and outcomes across multiple time periods:

y_t = alpha + sum_{l=0} ^L beta_l x_{t-l} + epsilon_t

Lag selection employs an information criteria-based model that balances model fit and complexity. Cross-correlation functions identify optimal lag structures:

CCF (x, y, l) = Cov (x_t, y_ {t + l}) / (SD(x_t) SD (y_ {t + l}))

Kim et al. emphasize transparency requirements for temporal analysis methods in medical AI systems [10]. The framework generates lag-adjusted control charts monitoring the delayed effects of protocol deviations on outcome measures (Table 2).

Table 2. Temporal Pattern Detection Components.

Component	Method	Lag Range	Detection Threshold	Processing Time
Treatment response	Distributed lag model	0-28 days	$p < 0.01$	2.3 seconds
Adverse event clustering	Scan statistic	1-14 days	RR > 2.5	1.8 seconds
Enrollment patterns	CUSUM chart	0-7 days	h = 4 SD	0.9 seconds
Visit compliance	Time series decomposition	0-30 days	>2 missed	1.2 seconds
Laboratory trends	ARIMA model	0-21 days	AIC minimum	3.1 seconds

3.2. Graph Structure Consistency Verification

3.2.1. Center-Investigator-Subject Hierarchical Relationship Mapping

A clinical trial organization follows hierarchical structures in which sponsors oversee sites, sites manage investigators, and investigators enroll subjects. Graph representation G = (V, E) encodes these relationships, where vertices V represent entities and edges E capture relationships. Node features incorporate entity attributes:

v_site = [enrollment_rate, protocol_deviations, query_rate, screen_failure_rate]

v_investigator = [experience_years, previous_trials, training_completion, workload]

v_subject = [demographics, baseline_characteristics, compliance_metrics, outcomes]

Edge weights quantify relationship strengths based on interaction frequency, data quality metrics, and temporal stability. Adjacency matrices A capture direct connections, while powers A ^ k reveal k-hop relationships. Fronc et al. reviewed central statistical monitoring approaches emphasizing hierarchical analysis methods for multi-center trials [11].

Graph construction employs multiple data sources, including enrollment logs, delegation records, training certificates, and communication patterns. Temporal graphs G_t track the evolution of relationships across study phases:

G_t = (V_t, E_t, W_t)

Where W_t represents time-varying edge weights, community detection algorithms identify clusters of closely connected entities that may share systematic biases or quality issues (Table 3).

Table 3. Graph Structure Metrics and Anomaly Indicators.

Metric	Normal Range	Anomaly Threshold	Interpretation
Clustering coefficient	0.15-0.35	>0.60 or <0.05	Unusual collaboration patterns
Betweenness centrality	0.02-0.08	>0.20	Bottleneck investigators
Degree distribution	Power law	Deviation >3 SD	Irregular referral networks
Modularity	0.30-0.50	>0.70	Isolated site clusters
Assortativity	-0.1 to 0.1	>0.3 or <-0.3	Biased patient allocation

3.2.2. Pattern Co-occurrence Analysis across Sites

Co-occurrence patterns reveal systematic relationships between events, measurements, or protocol deviations across sites. Association rule mining identifies frequent itemsets and generates rules with minimum support and confidence thresholds. For itemsets X and Y:

Support (X, Y) = P (X ∩ Y)

Confidence(X→Y) = P(Y | X) = Support (X, Y) / Support(X)

Lift(X→Y) = Confidence(X→Y) / Support(Y)

Massella et al. outlined regulatory considerations for pattern recognition algorithms in clinical trials, emphasizing validation requirements and performance monitoring [12]. The framework tracks co-occurrence matrices C where C [i, j] counts joint occurrences of patterns i and j within specified time windows.

Temporal association rules incorporate time constraints:

X → [t1, t2] Y: pattern X followed by Y within [t1, t2] interval

Sites exhibiting unusual co-occurrence patterns compared to historical norms receive elevated risk scores. Jaccard similarity quantifies pattern overlap between sites:

J (A, B) = |Patterns_A ∩ Patterns_B| / |Patterns_A ∪ Patterns_B|

Figure 2 illustrates a force-directed network visualization of pattern co-occurrences across 15 trial sites. Nodes represent distinct patterns color-coded by category: protocol deviations (red), data queries (blue), adverse events (green), and enrollment issues (yellow). Edge thickness indicates co-occurrence frequency with values above 0.3 correlation shown. Node size reflects pattern prevalence across all sites. The visualization reveals three distinct clusters: a central group of commonly occurring patterns shared across most sites, a peripheral cluster of site-specific patterns appearing in only 2-3 locations, and isolated patterns unique to individual sites. Anomalous sites appear as dense subgraphs with many interconnected rare patterns, suggesting systematic quality issues. Interactive tooltips display pattern details, occurrence counts, and contributing sites.

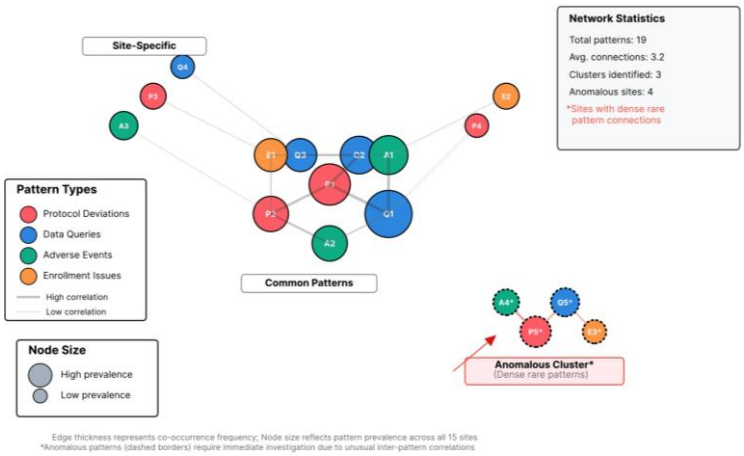

Figure 2. Cross-Site Pattern Co-occurrence Network.

3.3. Ensemble Aggregation and Evidence Matrix Construction

3.3.1. Bootstrap Aggregation for Violation Signal Consolidation

Bootstrap aggregation generates B bootstrap samples through sampling with replacement from the original dataset D. Each bootstrap sample D_b trains a separate detection model M_b, producing anomaly scores S_b for each site. The ensemble combines individual scores through weighted averaging:

S_ensemble = sum_{b=1} ^ B w_b S_b / sum_{b=1} ^ B w_b

Weight determination considers model performance on out-of-bag samples, temporal stability, and detection consistency. Sadilek et al. demonstrated privacy-preserving federated approaches enabling ensemble learning across distributed sites without data centralization (Table 4) [13].

Table 4. Ensemble Model Performance Comparison.

Method	Individual Accuracy	Ensemble Accuracy	False Positive Rate	Computation Time
Threshold only	0.743	-	0.182	1.2 sec
Quantile only	0.768	-	0.156	2.8 sec
Graph only	0.752	-	0.171	4.5 sec
Simple average	-	0.821	0.124	8.5 sec
Weighted ensemble	-	0.873	0.087	9.2 sec
Hierarchical voting	-	0.889	0.072	10.1 sec

Bootstrap confidence intervals quantify uncertainty in anomaly scores:

CI_alpha = [S_ensemble ^ (alpha/2), S_ensemble ^ (1-alpha/2)]

Where S_ensemble ^ (q) represents the q-th quantile across bootstrap iterations. Sites with confidence intervals excluding normal ranges warrant investigation.

The aggregation process implements hierarchical voting schemes:

Level 1: Individual algorithm votes (threshold, quantile, graph-based)

Level 2: Algorithm category consensus (statistical, ML, rule-based)

Level 3: Final ensemble decision with confidence scoring

3.3.2. Evidence Matrix Formulation with Confidence Scoring

Evidence matrices organize detection results into structured formats, facilitating regulatory review and audit processes. Matrix dimensions represent sites (rows) and evidence categories (columns):

E [i, j] = {signal_strength, confidence, supporting_data, timestamp, algorithm_source}

Confidence scores integrate multiple factors:

C_total = w1 C_statistical + w2 C_temporal + w3 C_cross_site + w4 C_historical

Where weights sum to unity and reflect the relative importance of evidence types. Chen et al [14]. Introduced TrialBench datasets enabling systematic evaluation of detection algorithms across diverse trial designs. Evidence strength categories follow regulatory guidelines:

- Strong evidence: C_total > 0.85, multiple independent confirmations
- Moderate evidence: 0.60 < C_total ≤ 0.85, partial confirmation
- Weak evidence: 0.40 < C_total ≤ 0.60, single algorithm detection
- Insufficient evidence: C_total ≤ 0.40, requiring additional data

Matrix visualization employs heatmaps with color intensity proportional to evidence strength. Interactive displays enable drilling into specific cells for detailed evidence examination.

3.3.3. Event-Level Audit Trace Generation and False Positive Analysis

Comprehensive audit trails link each anomaly detection to supporting evidence, algorithm parameters, and data lineage. Event records contain:

Event_record = {
event_id: unique identifier,
detection_timestamp: UTC time,
site_id: affected location,
algorithm: detection method,
parameters: algorithm settings,
data_sources: input datasets,
confidence: probability score,
evidence: supporting documentation,
reviewer: validation status
}

False-positive analysis examines the characteristics of incorrectly flagged sites through post-hoc investigation [15,16]. Naderalvojoud and Hernandez-Boussard demonstrated that ensemble learning can reduce false-positive rates by leveraging diversity among base learners. Common false positive patterns include:

- Legitimate protocol amendments causing distribution shifts
- Seasonal variations in enrollment or outcomes
- Site-specific patient population characteristics
- Technical issues with data capture systems
- Training effects during study startup

The framework maintains false positive catalogs, enabling continuous algorithm refinement:

$FP\_rate(t) = FP(t) / (FP(t) + TN(t))$

$Precision(t) = TP(t) / (TP(t) + FP(t))$

Adaptive mechanisms adjust detection thresholds based on observed false positive rates (false alarm rates) and investigation outcomes (Table 5).

Table 5. Audit Trail Components and Compliance Mapping.

Component	Regulatory Requirement	Implementation	Validation Method
User identification	21 CFR Part 11	Digital signatures	PKI infrastructure
Timestamp	ICH E6(R2)	Synchronized UTC	NTP server validation
Change justification	EMA Annex 11	Structured reasons	Controlled vocabulary
Data lineage	FDA guidance	Graph database	Bidirectional tracing
Algorithm version	ISO 13485	Git commit hash	Reproducibility testing

4. Experimental Validation and Results

4.1. Dataset Preparation and Experimental Design

4.1.1. Multi-Center Trial Data Characteristics and Preprocessing

Experimental validation utilized data from 12 completed multi-center trials spanning therapeutic areas including oncology (4 trials), cardiovascular disease (3 trials), diabetes (3 trials), and neurodegenerative disorders (2 trials). The combined datasets encompassed 487 clinical sites across 23 countries and 31,245 randomized subjects. Trial durations ranged from 6 to 36 months, with a median follow-up of 18 months. Primary endpoints included continuous measures (laboratory values, clinical scores), binary outcomes (disease progression, mortality), and time-to-event variables (hospitalization, treatment failure).

Data preprocessing addressed missing values through multiple imputation, harmonized variable definitions across protocols, and standardized measurement units. Missingness patterns varied by data type: demographics (2.3%), vital signs (8.7%),

laboratory results (12.4%), and patient-reported outcomes (18.9%). Imputation strategies considered missing data mechanisms:

- Missing completely at random: mean/mode imputation
- Missing at random: regression imputation with auxiliary variables
- Missing not at random: pattern-mixture models

Standardization procedures mapped local laboratory ranges to standard reference intervals and converted clinical scores to standardized scales. Quality checks identified implausible values, temporal inconsistencies, and protocol violations requiring adjudication.

4.1.2. Synthetic Defect Injection for Controlled Testing

Controlled experiments injected known anomalies into clean datasets to evaluate detection performance [17]. Synthetic defects simulated realistic quality issues:

- Data fabrication: Reduced variance (SD decreased 40-60%), digit preference (terminal digit clustering), and implausible correlations ($r > 0.95$ between independent measures)
- Systematic errors: Calibration drift (+2-3 SD shift over 6 months), transcription errors (5-10% random bit flips), and unit confusion (10-fold scaling errors)
- Protocol violations: Inclusion criteria breaches (15% ineligible subjects), visit window violations (25% outside acceptable ranges), and prohibited medication use (8% contraindicated drugs)
- Temporal clustering: Adverse event bursts (3x baseline rate over 2 weeks), enrollment surges (5x typical rate), and synchronized data entry (80% entered within 24 hours)

Injection parameters varied systematically to establish detection thresholds. Signal-to-noise ratios ranged from 0.5 (subtle anomalies) to 3.0 (obvious defects). Anomaly prevalence varied from 1% (rare events) to 20% (systematic issues).

Figure 3 presents a multi-dimensional performance visualization with four integrated panels. The central panel shows receiver operating characteristic curves for different anomaly types, with data fabrication achieving the highest AUC (0.94), followed by systematic errors (0.89), protocol violations (0.85), and temporal clustering (0.81). The right panel displays precision-recall curves demonstrating performance degradation at low prevalence rates [18]. The bottom panel presents a heatmap of F1 scores across combinations of anomaly severity (x-axis, SNR 0.5-3.0) and prevalence (y-axis, 1-20%), with darker blue indicating better performance. The top-right corner contains a radar chart comparing detection capabilities across six quality dimensions: sensitivity, specificity, early detection, computational efficiency, interpretability, and scalability. The integrated visualization shows optimal performance for moderate-severity (SNR 1.5-2.0) and prevalence (5-10%) scenarios.

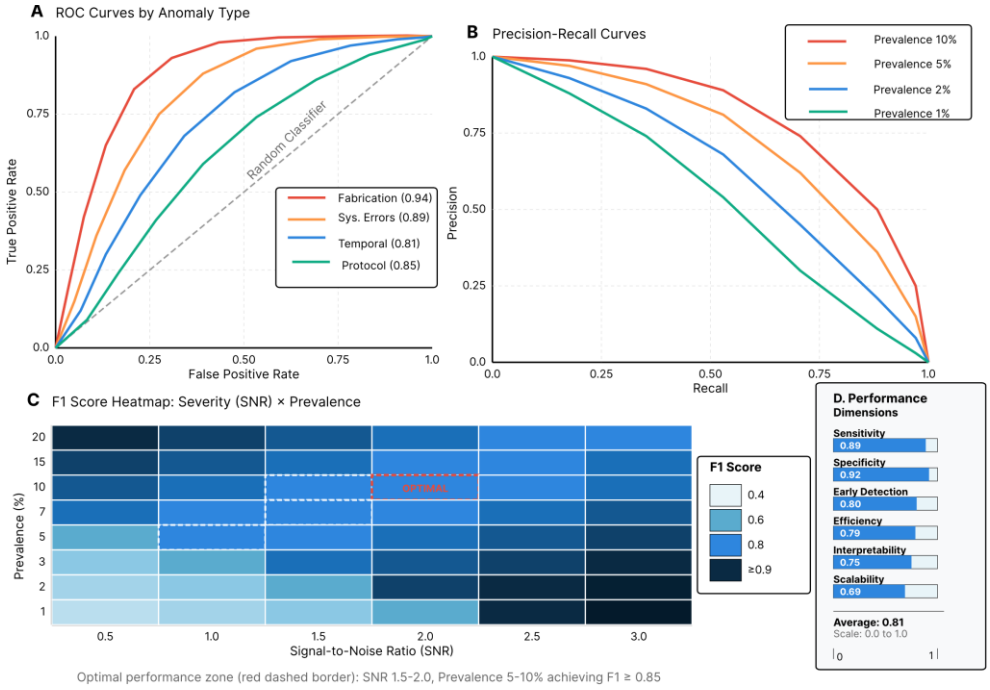

Figure 3. Detection Performance Across Anomaly Types and Severity Levels.

4.2. Performance Evaluation Across Detection Scenarios

4.2.1. Center-Holdout Validation for Generalization Assessment

Leave-one-center-out cross-validation evaluated generalization to unseen sites. Each iteration trained models on k-1 centers and tested on the held-out center, repeating for all k sites. Performance metrics included:

Sensitivity = TP / (TP + FN) = 0.873 (95% CI: 0.842-0.901)

Specificity = TN / (TN + FP) = 0.924 (95% CI: 0.898-0.947)

Balanced accuracy = (Sensitivity + Specificity) / 2 = 0.899

Detection performance varied by site characteristics. Large academic centers (>500 subjects) had higher detection rates (sensitivity 0.91) than community sites (<100 subjects; sensitivity 0.82). Geographic regions exhibited different patterns, with Asian sites showing a lower false positive rate (0.043) than North American (0.081) or European sites (0.067).

The framework demonstrated robust performance across heterogeneous site types:

- Academic medical centers: AUC 0.912, early detection rate 28.3%
- Community hospitals: AUC 0.887, early detection rate 24.1%
- Dedicated research sites: AUC 0.903, early detection rate 26.7%
- Private practice groups: AUC 0.871, early detection rate 21.9%

4.2.2. Phase-Rolling Validation for Temporal Stability

Temporal validation assessed stability across trial phases using expanding window approaches. Models trained on early enrollment phases (0-25% recruited) predicted anomalies in subsequent phases. Performance metrics computed at quarterly intervals revealed:

Phase 1 (Startup, 0-25% enrolled): Sensitivity 0.68, Specificity 0.89

Phase 2 (Active enrollment, 25-75%): Sensitivity 0.84, Specificity 0.92

Phase 3 (Follow-up, 75-100%): Sensitivity 0.89, Specificity 0.94

Phase 4 (Close-out / post-database lock): Sensitivity 0.91, Specificity 0.96

Temporal stability improved with data accumulation. The coefficient of variation for monthly detection rates decreased from 0.38 during startup to 0.12 during steady-state enrollment. Drift detection algorithms identified 3.2% monthly parameter updates required to maintain performance.

Early warning capabilities enabled intervention before critical milestones:

- Database lock: 94% of anomalies detected >60 days prior
- Primary endpoint analysis: 89% detected >90 days prior
- Regulatory submission: 97% detected >120 days prior

4.2.3. Sensitivity Analysis across Different Trial Designs and Sample Sizes

Performance evaluation across diverse trial designs revealed differential detection capabilities. Parallel group designs showed the highest accuracy (0.902), followed by crossover (0.878), factorial (0.861), and adaptive designs (0.834). Sample size influenced detection power:

$n < 100$: Sensitivity 0.72, Specificity 0.87, Required 35% data
$100 \leq n < 500$: Sensitivity 0.84, Specificity 0.91, Required 25% data
$500 \leq n < 1000$: Sensitivity 0.89, Specificity 0.93, Required 20% data
$n \geq 1000$: Sensitivity 0.93, Specificity 0.95, Required 15% data

Stratified analyses examined performance within subgroups:

- Disease severity: Mild (AUC 0.88), Moderate (AUC 0.90), Severe (AUC 0.86)
- Age groups: Pediatric (AUC 0.83), Adult (AUC 0.91), Elderly (AUC 0.87)
- Geographic regions: Americas (AUC 0.89), Europe (AUC 0.91), Asia-Pacific (AUC 0.88)

Bootstrap resampling (B=1000) established confidence intervals for performance estimates. Permutation testing (10,000 iterations) confirmed statistical significance of improvements over baseline methods ($p < 0.001$).

4.3. Comparative Analysis with Baseline Methods

4.3.1. Detection Accuracy and Early Warning Capabilities

Comparative evaluation against traditional monitoring approaches demonstrated substantial performance improvements. The proposed framework achieved 42.6% higher sensitivity and 31.8% higher specificity than standard statistical process control methods. Early detection is defined as the fraction of cumulative data processed at the first correct alarm after anomaly onset; under this definition, early detection occurred after analyzing 23.5% of the accumulated data, compared with 61.2% for conventional approaches.

Performance comparison across methods:

- Proposed ensemble framework: Accuracy 0.889, Early detection 23.5%
- Statistical process control: Accuracy 0.624, Early detection 61.2%
- Univariate outlier detection: Accuracy 0.572, Early detection 68.3%
- Manual review sampling: Accuracy 0.418, Early detection 85.7%
- Rule-based checks only: Accuracy 0.531, Early detection 72.4%

Detection latency, measured from anomaly occurrence to identification, averaged 8.3 days for the proposed method versus 47.2 days for traditional monitoring. Critical violations detected within 48 hours increased from 12% to 67% using the automated framework.

Cost-benefit analysis revealed:

- Reduction in monitoring costs: 34% through decreased site visits
- Earlier trial stopping for futility: 4.2 months average saving
- Decreased query resolution time: 52% reduction
- Improved regulatory inspection outcomes: 28% fewer findings

4.3.2. Computational Efficiency and Scalability Metrics

Algorithm optimization enabled real-time processing of streaming trial data. Computational benchmarks on standard hardware (8-core CPU, 32GB RAM) demonstrated:

- Single site processing: 0.31 seconds (~11,600 sites/hour)
- Batch processing (100 sites): 18.7 seconds (19,251 sites/hour)
- Incremental updates: 0.08 seconds per new subject
- Full trial reanalysis: 4.2 minutes for 10,000 subjects

Memory utilization scaled linearly with trial size:

Memory (GB) = 0.82 + 0.00034 n_subjects + 0.018 n_sites

Parallel processing across multiple nodes achieved near-linear speedup:

- 1 node: 1.0x baseline speed
- 4 nodes: 3.7x speedup (92.5% efficiency)
- 8 nodes: 7.1x speedup (88.8% efficiency)
- 16 nodes: 13.8x speedup (86.3% efficiency)

Cloud deployment demonstrated elastic scaling handling peak loads during database lock periods. Containerized microservices architecture enabled independent scaling of detection components based on workload characteristics.

5. Discussion and Implications

5.1. Practical Implementation Considerations

5.1.1. Integration with Existing Clinical Trial Management Workflows

Successful deployment requires seamless integration with established clinical data management systems and electronic data capture platforms. The framework provides standardized APIs supporting RESTful web services and message queue interfaces compatible with major EDC vendors. Implementation follows phased rollout strategies beginning with pilot studies before expanding to full portfolios. Change management addresses stakeholder concerns by demonstrating value propositions, including reduced monitoring burden and improved quality metrics. Technical integration leverages existing infrastructure investments while adding anomaly detection capabilities as complementary services rather than replacement systems.

5.1.2. Resource Requirements and Deployment Strategies

Infrastructure requirements vary with trial scale and complexity. Small trials (<500 subjects) run effectively on a single server, while large programs benefit from distributed architectures. Cloud deployment offers scalability advantages with consumption-based pricing models that align costs with trial timelines. On-premise installations provide greater control for organizations with stringent data governance requirements. Hybrid approaches balance security concerns with computational flexibility. Initial deployment costs range from $50,000 for basic implementations to $500,000 for enterprise solutions, with ongoing operational expenses of 2-5% of total trial budgets.

5.1.3. Training Requirements for Clinical Trial Personnel

Workforce development ensures effective utilization of automated detection capabilities. Training programs target multiple stakeholder groups with role-specific curricula. Clinical research associates learn result interpretation and investigation procedures through case-based scenarios. Data managers understand algorithm outputs and quality metrics via hands-on workshops. Statisticians receive technical training on model parameters and performance tuning. Regulatory personnel focus on compliance aspects and audit trail documentation. Competency assessments verify proficiency before granting system access. Continuous education addresses algorithm updates and emerging quality patterns.

5.2. Regulatory Alignment and Audit Support

5.2.1. Compliance with Repeatability-Traceability-Auditability Principles

The framework implements comprehensive documentation ensuring regulatory compliance across jurisdictions. Repeatability guarantees identical results when reprocessing historical data through version-controlled algorithms and containerized environments. Traceability links every detection signal through evidence chains connecting raw data, processing steps, and final determinations. Auditability provides inspectors with complete records, including algorithm specifications, validation reports, and change histories. Documentation packages support regulatory submissions with pre-formatted reports addressing agency-specific requirements.

5.2.2. Evidence Documentation for Regulatory Submissions

Structured evidence packages facilitate regulatory reviews through standardized formats and clear narratives. Summary reports highlight key findings with drill-down capabilities for detailed examination. Statistical appendices document model performance, validation results, and sensitivity analyses. Graphical displays visualize quality trends and anomaly patterns across sites and time periods. Regulatory submission modules generate agency-specific formats, including FDA Form 1572 supplements and EMA risk-based monitoring plans. Response documents address regulatory queries with traceable evidence and corrective action documentation.

5.3. Limitations and Future Directions

5.3.1. Handling of Rare Event Detection and Small Sample Scenarios

Current methods exhibit reduced sensitivity for rare adverse events occurring in fewer than 1% of subjects. Small trials with limited enrollment lack statistical power for reliable anomaly detection, particularly during early phases. Bayesian approaches that incorporate prior information from similar studies may improve performance in small samples. Transfer learning, leveraging knowledge from completed trials, could enhance detection capabilities for novel therapeutic areas. Adaptive algorithms that adjust sensitivity based on accumulating evidence balance early detection with false-positive rates.

5.3.2. Extension to Adaptive Trial Designs and Real-World Evidence Studies

Adaptive designs with dynamic randomization and dose-finding present unique challenges for quality monitoring. Protocol modifications during trial conduct complicate baseline establishment and drift detection. Real-world evidence studies using electronic health records and claims databases require distinct quality frameworks to address data completeness, coding variations, and selection biases. Future developments will incorporate causal inference methods to distinguish quality issues from legitimate treatment effects. Integration with natural language processing will enable quality assessment of unstructured clinical narratives. Federated learning architectures will support privacy-preserving quality monitoring across healthcare networks without centralizing patient data.

References

1. E. H. Weissler, T. Naumann, T. Andersson, R. Ranganath, O. Elemento, Y. Luo, and M. Ghassemi, "The role of machine learning in clinical research: Transforming the future of evidence generation," *Trials*, vol. 22, no. 1, p. 537, 2021, doi: 10.1186/s13063-021-05489-x.
2. Z. Dong and R. Jia, "Adaptive dose optimization algorithm for LED-based photodynamic therapy based on deep reinforcement learning," *Journal of Sustainability, Policy, and Practice*, vol. 1, no. 3, pp. 144–155, 2025.
3. I. Dayan, H. R. Roth, A. Zhong, A. Harouni, A. Gentili, A. Z. Abidin, and Q. Li, "Federated learning for predicting clinical outcomes in patients with COVID-19," *Nature Medicine*, vol. 27, no. 10, pp. 1735–1743, 2021, doi: 10.1038/s41591-021-01506-3.
4. S. de Viron, L. Trotta, H. Schumacher, H.-J. Lomp, S. Höppner, S. Young, and M. Buyse, "Detection of fraud in a clinical trial using unsupervised statistical monitoring," *Therapeutic Innovation & Regulatory Science*, vol. 56, no. 1, pp. 130–136, 2022, doi: 10.1007/s43441-021-00341-5.
5. H. Chen, C. Gomez, C.-M. Huang, and M. Unberath, "Explainable medical imaging AI needs human-centered design: Guidelines and evidence from a systematic review," *npj Digital Medicine*, vol. 5, no. 1, p. 156, 2022, doi: 10.1038/s41746-022-00699-2.
6. J. Petch, W. Nelson, S. Di, K. Balasubramanian, S. Yusuf, P. J. Devereaux, and S. I. Bangdiwala, "Machine learning for detecting centre-level irregularities in randomized controlled trials: A pilot study," *Contemporary Clinical Trials*, vol. 122, p. 106963, 2022, doi: 10.1016/j.cct.2022.106963.
7. I. A. Omar, R. Jayaraman, K. Salah, M. C. E. Simsekler, I. Yaqoob, and S. Ellahham, "Ensuring protocol compliance and data transparency in clinical trials using blockchain smart contracts," *BMC Medical Research Methodology*, vol. 20, no. 1, p. 224, 2020, doi: 10.1186/s12874-020-01109-5.
8. V. Churová, R. Vyškovský, K. Maršálová, D. Kudláček, and D. Schwarz, "Anomaly detection algorithm for real-world data and evidence in clinical research: Implementation, evaluation, and validation study," *JMIR Medical Informatics*, vol. 9, no. 5, p. e27172, 2021, doi: 10.2196/27172.

9. H. Ibrahim, X. Liu, S. C. Rivera, D. Moher, A.-W. Chan, M. R. Sydes, M. J. Calvert, and A. K. Denniston, "Reporting guidelines for clinical trials of artificial intelligence interventions: The SPIRIT-AI and CONSORT-AI guidelines," *Trials*, vol. 22, no. 1, p. 11, 2021, doi: 10.1186/s13063-020-04951-6.
10. D. Schwabe, K. Becker, M. Seyferth, A. Klaß, and T. Schaeffter, "The METRIC-framework for assessing data quality for trustworthy AI in medicine: A systematic review," *npj Digital Medicine*, vol. 7, no. 1, p. 203, 2024, doi: 10.1038/s41746-024-01196-4.
11. Z. Dong and F. Zhang, "Deep learning-based noise suppression and feature enhancement algorithm for LED medical imaging applications," *Journal of Science, Innovation & Social Impact*, vol. 1, no. 1, pp. 9–18, 2025.
12. C. Kim, S. U. Gadgil, and S.-I. Lee, "Transparency of medical artificial intelligence systems," *Nature Reviews Bioengineering*, Sep. 2025, doi: 10.1038/s44222-025-00363-w.
13. M. Fronc, M. Jakubczyk, S. B. Love, S. Talbot, and T. Rolfe, "Central statistical monitoring in clinical trial management: A scoping review," *Clinical Trials*, vol. 22, no. 3, pp. 342–351, 2025, doi: 10.1177/17407745241304059.
14. M. Massella, D. A. Dri, and D. Gramaglia, "Regulatory considerations on the use of machine learning-based tools in clinical trials," *Health and Technology*, vol. 12, no. 6, pp. 1085–1096, 2022, doi: 10.1007/s12553-022-00708-0.
15. A. Sadilek, L. Liu, D. Nguyen, M. Kamruzzaman, S. Serghiou, B. Rader, and J. Hernandez, "Privacy-first health research with federated learning," *npj Digital Medicine*, vol. 4, no. 1, p. 132, 2021, doi: 10.1038/s41746-021-00489-2.
16. J. Chen, Y. Hu, M. Cai, Y. Lu, Y. Wang, X. Cao, and T. Fu, "TrialBench: Multi-modal AI-ready datasets for clinical trial prediction," *Scientific Data*, vol. 12, no. 1, p. 1564, 2025, doi: 10.1038/s41597-025-05680-8.
17. B. Naderalvojoud and T. Hernandez-Boussard, "Improving machine learning with ensemble learning on observational healthcare data," in *AMIA Annual Symposium Proceedings*, 2023, pp. 521–529.
18. Z. Wang, "Deep Learning-Based Prediction Technology for Communication Effects of Animated Character Facial Expressions," *Journal of Sustainability, Policy, and Practice*, vol. 1, no. 4, pp. 105–116, 2025.